

**Modeling three-dimensional cohesive sediment transport  
and associated morphological variation in estuarine intertidal mudflats**

**Yusuke UCHIYAMA**

**March 2005**

**Littoral Drift Division  
Port and Airport Research Institute  
Yokosuka, JAPAN**

## **Modeling three-dimensional cohesive sediment transport and associated morphological variation in estuarine intertidal mudflats**

**Yusuke UCHIYAMA\***

### **Synopsis**

A numerical model has recently been developed with incorporating a wetting and drying scheme into the Princeton Ocean Model (POM; Blumberg and Mellor, 1983) to simulate tidal currents in San Francisco Bay, CA, USA (WD-POM; Uchiyama, 2004). San Francisco Bay is encompassed by extensive intertidal area including mudflats and salt marshes where flooding and draining are predominant for overlaying hydrodynamics. Intertidal sediment transport and associated topography changes are of interest for coastal engineers (e.g., Dyer, 1986) as well as marine biologists (e.g., Kuwae *et al.*, 2003), whereas no three-dimensional numerical models have been developed thus far to calculate the intertidal sediment transport properly. In the present study, cohesive sediment transport and bed elevation changes are modeled and adapted to WD-POM to assess intertidal morphodynamics in San Francisco Bay.

The cohesive sediment transport model contains settling speeds of cohesive flocs (Burban *et al.*, 1990) and the sink/source terms due to deposition (Partheniades, 1992) and resuspension (Krone, 1962) at the seabed. The governing equation is transformed into the horizontal orthogonal curvilinear coordinate and the vertical sigma coordinate as used in WD-POM. The bed elevation model is also developed based upon the volume conservation of the deposited/suspended sediments and is capable of considering consolidation through sediment porosity.

Astronomical tidal oscillations are imposed onto the open boundary condition off Golden Gate (the bay mouth). Neither fluvial sediments nor surface wind stresses are assumed in the computation for the simplicity. The model outputs exhibit that cohesive sediments are suspended dominantly in the deeper channels while being transported and deposited on intertidal areas fringing the bay. The morphological change due to tidal currents during two spring-neap cycles shows that intertidal mudflats tend to slightly be accreted yet channels seem rather eroded. These results demonstrate that the intertidal areas play an important role in the sediment budgets in the estuary, acting as 'sink' of the suspended cohesive sediments under action of the tidal currents.

**Key Words:** cohesive sediment transport, morphological change, intertidal mudflat, numerical model

---

\* Senior Researcher, Littoral Drift Division, Marine Environment and Engineering Department  
3-1-1 Nagase, Yokosuka 239-0826, Japan  
phone: +81-46-844-5045, facsimile: +81-46-841-9812, email: uchiyama@pari.go.jp

## 内湾干潟海域における3次元凝集性土砂輸送 およびそれに伴う地形変動のモデリング

内山 雄介\*

### 要 旨

代表的な 3 次元海洋流動モデルである Princeton Ocean Model (POM; Blumberg and Mellor, 1983) に適用可能な冠水・干出スキームが著者によって開発され、米国サンフランシスコ湾の潮流シミュレーションに適用された (WD-POM; Uchiyama, 2004) . WD-POM では新たに拡張対数則が導入され、潮間帯周辺において水深が極めて浅くなった場合であっても、海底面境界層内外の流速分布構造、および底質再懸濁に対して重要な底面シアをより正確に再現することが可能となっている。サンフランシスコ湾は広大な潮間帯・干潟により沿岸部を囲まれた典型的な閉鎖性内湾であり、干出・冠水現象が湾内流動に対して重要な役割を果たしている。このような潮間帯域における底質輸送とそれに伴う地形変化の機構と実態については、海岸工学分野 (例えば, Dyer, 1986) だけではなく、海洋生物分野 (例えば, Kuwae *et al.*, 2003) においても注目されている。しかしながら、潮間帯域の底質輸送を精緻に再現する 3 次元モデルはこれまで提案されていなかった。そこで本研究では、WD-POM に適用可能な 3 次元凝集性土砂 (cohesive sediment) 輸送モデルおよび地形変化モデルを開発し、それらをサンフランシスコ湾に適用して湾内の底質移動、海底地形変動特性を検討する。

土砂輸送モデルは沈降速度を考慮した 3 次元の移流拡散方程式を基礎式とし、水塊のシアと凝集性土砂のフロック形成を考慮した沈降速度 (Burban *et al.*, 1990) , 海底面における沈降堆積速度 (Partheniades, 1992) および再懸濁侵食速度 (Krone, 1962) の各サブモデルが含まれている。基礎方程式は WD-POM に適合するように 3 次元デカルト座標系から水平直交曲線座標系および鉛直  $\sigma$  座標系へと変換されている。海底地形変動モデルは底質の沈降、再懸濁を考慮した海底面における土砂の体積保存則に基いており、底質の間隙率を通じて圧密沈下を考慮できるように定式化されている。

湾口部 (Golden Gate 西側) の開境界において、天文潮のみを与えて湾内の潮流分布およびそれに伴う土砂輸送と地形変化に関する計算を行った。本研究では潮流成分による土砂輸送の効果を検討するため、湾北東部の Sacramento-San Joaquin デルタからの淡水流入や、海表面における風応力の作用 (吹送流および風波) は考慮していない。モデルによる計算結果から、凝集性土砂の再懸濁は湾中央に形成された水深の深い水路部において卓越しており、下げ潮流によって潮間帯周辺を含む浅海域方向に土砂が輸送されて沈降するというメカニズムが卓越することが明らかとなった。これに対応して、二朔望周期 (約 28 日間) における潮流による地形変化結果から、水路部では侵食が、潮間帯干潟では堆積が卓越していることが分かった。すなわち、潮間帯干潟域は内湾全体の流動だけではなく土砂収支の観点からも非常に重要な役割を果たしており、潮流に対しては土砂の“シンク”として機能していることが示された。

キーワード：凝集性土砂輸送，地形変化，潮間帯干潟，数値モデル

---

\* 海洋・水工部 漂砂研究室 主任研究官

〒239-0826 神奈川県横須賀市長瀬3-1-1

電話：046-844-5045, FAX：046-841-9812, Eメール：uchiyama@pari.go.jp

## CONTENTS

<b>Synopsis</b> .....	1
<b>1. INTRODUCTION</b> .....	5
<b>2. STUDY SITE</b> .....	6
<b>3. NUMERICAL MODELING</b> .....	7
3.1. Cohesive Sediment Transport.....	7
3.2. Boundary Conditions and Empirical Submodels.....	8
3.3. Bed Shear Stress and Vertical Mixing Parameterization.....	8
3.4. Bed Elevation Modeling.....	9
<b>4. RESULTS</b> .....	9
4.1. Cohesive Sediment Concentrations.....	9
4.2. Geomorphological Variations.....	12
<b>5. DISCUSSION</b> .....	14
<b>6. CONCLUSIONS</b> .....	15
<b>ACKNOWLEDGEMENTS</b> .....	15
<b>REFERENCES</b> .....	15



## 1. INTRODUCTION

Intertidal mudflats play a crucial role in the transport of land-sourced sediments and contaminants into estuaries. Currents and waves interact to erode mudflats and vary with tidal range, seasons, and episodic events such as storms. Sedimentation occurs during relatively calm periods, when accretion is higher than erosion (Christie and Dyer, 1998; Uchiyama *et al.*, 2001; Talke and Stacey, 2003). Mudflats are recognized to be an important component of the estuarine system, particularly with regard to sediments, contaminants, and organic matter because they provide an extensive boundary condition (Dyer, 1998). Hydrodynamics, sediment transport and associated morphological variations have been investigated mostly through field measurement programs particularly during the late 1990's (e.g., Wood *et al.*, 1998; Whitehouse and Mitchener, 1998; Widdows *et al.*, 1998; Li and Parchure, 1998; Van der Lee, 1998; Van der Lee, 2000; Whitehouse *et al.*, 2000). Intertidal sediment transport and associated topography changes are of interest not only for coastal engineers and physical oceanographers (e.g., Dyer, 1986) but also aquatic biochemists and marine biologists (e.g., Kerner, 1993; de Jonge and van Beusekom, 1995; Asmus *et al.*, 1998; Kuwae *et al.*, 1998; Cabrita and Brotas, 2000; Christensen *et al.*, 2000; Kuwae *et al.*, 2003)

Effort has also been made to develop numerical models for intertidal areas while wetting and drying (emergence during high waters and immergence during low waters) are essential to the intertidal hydrodynamics but it is generally difficult to implement the wetting/drying capability into three-dimensional numerical models. Nevertheless, a number of cohesive sediment transport models have been developed involving Sheng and Lick (1979), Thomas and McAnally (1985), Zeigler and Lick (1988), Hayter and Pakala (1989), Barros and Baptista (1989), Lee *et al.* (1994), Ziegler and Nisbet (1994, 1995), McDonald and Cheng (1997), Shrestha *et al.* (2000), Inagaki (2000), HydroQual Inc. (2002), Nakagawa (2003, 2005), Bricker *et al.* (2004), and others. Most of them are based on 2DH hydrodynamic models such as TRIM (Cheng *et al.*, 1993) which can readily be applied to intertidal simulations (McDonald and Cheng,

1997). However, intertidal mudflats extend in the estuaries where baroclinic motion is effectively significant for the hydrodynamics (Ralston and Stacey, 2004), and thus three-dimensional prognostic models are requisite for exploring intertidal sediment transport. Among the models referred to above, Inagaki (2000), Nakagawa (2003, 2005), and Bricker *et al.* (2004) developed the three-dimensional intertidal cohesive sediment transport models. Inagaki (2000) and Bricker *et al.* (2004) used a model based upon TRIM-3D (Casulli and Cattani, 1994; Gross *et al.*, 1998) which is originally capable of simulating inundation and drainage occurred on intertidal mudflats. However, both of them paid no attention to intertidal processes, whereas the simulations are done for South San Francisco Bay which is fringed by extensive intertidal areas and man-made salt ponds (Siegel and Bachand, 2002). Nakagawa (2003, 2005) employed the PHRI siltation model developed by Tsuruya *et al.* (1990) with implementing a wetting and drying capability to simulate cohesive sediment transport in Ariake Bay, Japan, still he mentioned nothing about effects of the intertidal mudflats surrounding the estuary on its hydrodynamics and sediment transport.

A wetting and drying scheme (WDS) has recently been developed and incorporated into the Princeton Ocean Model (POM; Blumberg and Mellor, 1983, 1987) to simulate tidal currents in San Francisco Bay (WD-POM; Uchiyama, 2004). The WDS is different from the other schemes proposed by Zheng *et al.* (2003), Xie *et al.* (2004), and Oey (2005) in representation of bed boundary layer since the extended logarithmic law was newly introduced into the WDS so as to accurately estimate bed shear stresses and resultant sediment resuspension and deposition in extremely shallow basins such as intertidal mudflats. The accuracy of WD-POM was verified by comparing the observed tidal surface elevations and 3D current velocities to the model outputs. The primary advantage of WD-POM over TRIM-3D and the PHRI model is its ability to evaluate the 3D hydrodynamics and associated scalar (salinity, temperature, sediments, etc.) transport even though water depth approaches zero in response to tide. This is mainly due to the coordinate systems that these models employ. Although TRIM-3D and the PHRI model are configured on

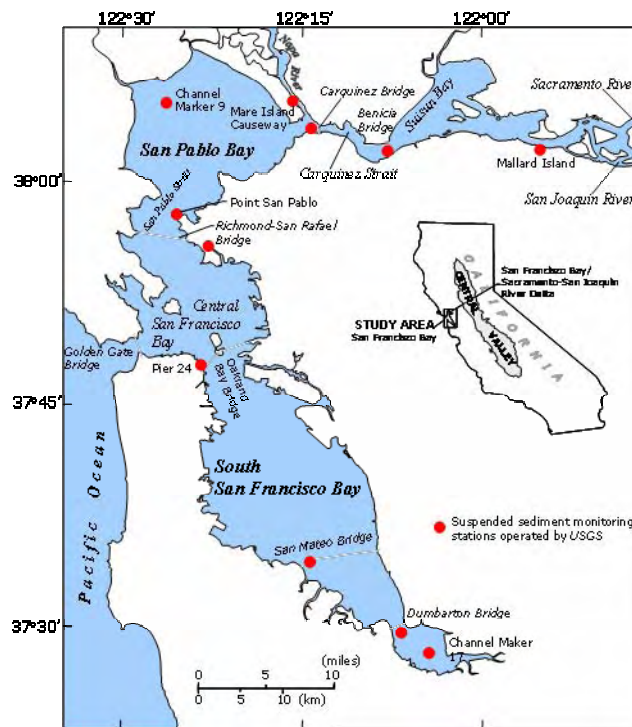


**Figure 1:** Location of the study: San Francisco Bay & Sacramento-San Joaquin Delta system, California, USA. Circle marks correspond to the turbidity measurement sites by Buchanan and Ruhl (2001) summarized in **Table 3**.

the 3D Cartesian coordinate with a so-called the multi-level vertical coordinate (where vertical grids are aligned parallel to a certain datum plane), WD-POM (and also its original version of POM) is on the 2DH orthogonal curvilinear coordinate with the vertical terrain-following sigma-coordinate (Uchiyama, 2004). The important conclusion of the study by Uchiyama (2004) is that in San Francisco Bay the intertidal mudflats are found to remarkably alter and control hydrodynamics of the embayment since the intertidal sloping bathymetry apparently enhances refraction and shoaling of propagating tidal waves while attenuating propagating speeds and consequent phases owing to increasing bed friction in the shallow regions.

The objectives of the present paper are to model cohesive sediment transport and associated morphological variations, to incorporate them into WD-POM, and to examine effects of intertidal topography on estuarine hydrodynamics and resultant sediment transport processes. Cohesive sediments are intricately influenced by ambient hydrodynamics, pore water dynamics, biostabilization, and bioturbation as reviewed in Black *et al.* (2002). To

avoid this complexity, the model presented here simply formulated by using the standard parameterizations such as by Krone (1962) for the resuspension rate, by Partheniades (1992) for the deposition rate, and by Burban *et al.* (1990) for the settling speeds. Attempts are made to extract some crucial properties of sedimentary dynamics from the computational results by paying careful attention to effects of the intertidal shallow topography.

## 2. STUDY SITE

San Francisco Bay, California, USA (**Figures 1 and 2**), consisting of South Bay, Central Bay, San Pablo Bay, and Suisun Bay, is chosen for the study site. The bay is a tidally-forced, semi-enclosed estuary encompassed by wide-spreading intertidal area comprising mudflats and salt marshes, where flooding and draining are predominant for overlaying hydrodynamics. San Francisco Bay has the surface area of about 1240km<sup>2</sup> and the intertidal mudflats of about 200km<sup>2</sup>. The Sacramento-San Joaquin delta system enormously supplies the freshwater and associated sediment influx sourced by the Sierra

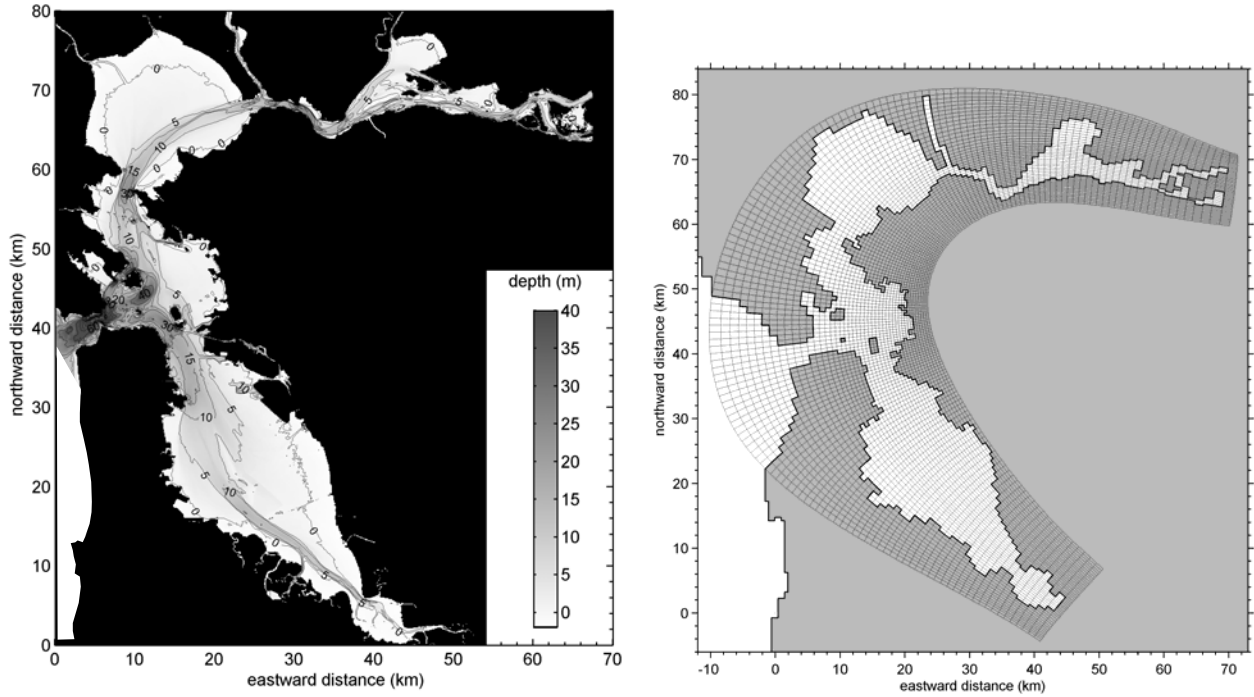


**Figure 2:** The bathymetric map of San Francisco Bay, California, USA (left) and the computational grid alignment using the horizontal orthogonal curvilinear transformation (right). The bathymetry is relative to the MLLW level.

Mountains and Central Valley to the northeastern part of the bay, i.e., Suisun Bay, San Pablo Bay and Central Bay. (Conomos *et al.* 1985). By contrast, South Bay, the southernmost part of San Francisco Bay, is often described as "a tidally oscillating lagoon with density-driven exchanges with the northern reach" (Gross *et al.*, 1999). Limited number of numerical simulations have been performed for San Francisco Bay by Cheng *et al.* (1993) and McDonald and Cheng (1997) using TRIM-2D, by Gross *et al.* (1998), Inagaki (2000) and Bricker *et al.* (2004) with TRIM-3D, and by Uchiyama (2004) with WD-POM, since emersion and immersion are indispensable to hydrodynamics of the embayment although generally laborious to incorporate into 3D hydrodynamic models.

### 3. NUMERICAL MODELING

#### 3.1 Cohesive Sediment Transport

Princeton Ocean Model (Blumberg and Mellor, 1983, 1987) consists of a set of the 3D primitive equations, Mellor-Yamada level 2.5 turbulent closure model (Mellor and Yamada, 1982; Galperin *et al.*, 1988) for vertical

eddy coefficients, and a Smagorinsky-type parameterization for horizontal mixing with the Boussinesq approximation and hydrostatic assumption. The governing equations are converted from the 3D Cartesian coordinate into the orthogonal curvilinear coordinate (horizontal) and  $\sigma$ -coordinate (vertical) to smoothly follow complex terrain geometries and marine bathymetries as shown in **Figure 2**. A wetting and drying feature is implemented by Uchiyama (2004) to deal with hydrodynamics in extremely shallow basins composed of intertidal flats and salt marshes. The cohesive sediment transport model to be coupled with WD-POM is developed here as expressed in Eqn. (1).

$$\frac{\partial CD}{\partial t} + \frac{\partial UCD}{\partial x} + \frac{\partial VCD}{\partial y} + \frac{\partial(\omega - W_s)C}{\partial \sigma} = \frac{\partial}{\partial \sigma} \left[ \frac{K_H}{D} \frac{\partial C}{\partial \sigma} \right] + F_C, \quad (1)$$

where  $(U, V, \omega)$ : 3D velocity vector,  $D$ : total depth ( $=H+\eta$ ,  $H$ : depth,  $\eta$ : surface elevation),  $C$ : cohesive sediment concentration,  $W_s$ : settling velocity,  $K_H$ : vertical eddy diffusivity, and  $F_C$ : the horizontal diffusion terms. Equation (1) is converted from the regular Cartesian coordinate into the 2D horizontal curvilinear and

**Table 1:** Summary of the hydrodynamic and numerical parameters used in the San Francisco Bay-simulation.

definition	parameter	value
time step for external mode (2D)	$\Delta t_e$	5 s
time step for internal mode (3D)	$\Delta t_i$	50 s
Smagorinsky constant	$A_M$	0.2
density of seawater	$\rho$	1025 kg/m <sup>3</sup>
roughness height	$z_0$	1 cm
critical depth used in WDS*	$d_{cr}$	20 cm
minimum depth used in WDS*	$d_{min}$	5 cm
scaling factor used in WDS*	$\delta$	1 cm

(\* see Uchiyama, 2004)

**Table 2:** Sedimentological parameters used in the San Francisco Bay-simulation.

definition	parameter	value
initial sediment concentration	$C _{t=0}$	0 mg/l
roughness height for sediments	$z_b$	0.5 cm
dry density of sediments	$\rho_s$	2.0 kg/m <sup>3</sup>
porosity of sediments	$\lambda_s$	0.5
minimum $\tau_b$ for erosion	$\tau_{be}$	0.15 Pa
minimum $\tau_b$ for deposition	$\tau_{bd}$	0.03 Pa
constant erosion probability	$P_e$	$5 \times 10^{-6}$ kg/m <sup>2</sup> /s

vertical sigma coordinate as used in WD-POM. Settling velocity,  $W_s$ , is unchanged in Eqn. (1) after the conversion into a  $\sigma$ -coordinate system (Wang, 2001; 2002). The horizontal advection terms (the second and third terms in the left hand side) are calculated with the Smolarkiewicz's iterative upstream scheme (Smolarkiewicz, 1984). All the terms in Eqn. (1) are solved explicitly except the vertical diffusion term.

### 3.2 Boundary Conditions and Empirical Sub-models

The boundary conditions for Eqn. (1) at the surface and seabed are defined as:

$$\frac{K_H}{D} \left( \frac{\partial C}{\partial \sigma} \right) = 0, \quad \sigma \rightarrow 0 \quad \text{at sea surface,} \quad (2)$$

$$\frac{K_H}{D} \left( \frac{\partial C}{\partial \sigma} \right) = E_r - D_p, \quad \sigma \rightarrow -1 \quad \text{at seabed,} \quad (3)$$

where  $E_r$ ,  $D_p$ : erosion and deposition rates at the seabed empirically formulated. The source term,  $E_r$ , is simplistically evaluated to represent resuspension of cohesive sediments from the bed in accordance with the conventional formulation using the threshold stress,  $\tau_{be}$ , for

the bed shear stress  $\tau_b$  and a constant erosion probability  $P_e$  (Krone, 1962; Ariathurai and Krone, 1976).

$$\begin{cases} E_r = P_e \left( \frac{\tau_b - \tau_{be}}{\tau_{be}} \right) & \text{when } \tau_b \geq \tau_{be} \\ E_r = 0 & \text{when } \tau_b < \tau_{be} \end{cases} \quad (4)$$

where  $P_e$ : the constant erosion probability,  $\tau_{be}$ : the critical bottom shear stress for erosion. Similarly, the sink term,  $D_p$ , in Eqn. (3) can be calculated by using the parameterization by Partheniades (1992).

$$D_p = W_s C P_d, \quad (5.1)$$

$$P_d = 1 - \frac{1}{\sqrt{2\pi}} \int_{-\infty}^Y e^{-\frac{\omega_0^2}{2}} d\omega_0, \quad (5.2)$$

$$Y = 2.04 \cdot \log \left[ 0.25 \left( \frac{\tau_b}{\tau_{bd}} - 1 \right) e^{1.27 \cdot \tau_{bd}} \right], \quad (5.3)$$

where  $P_d$ : the deposition probability,  $\omega_0$ : a dummy variable and  $\tau_{bd}$ : the bottom shear stress below which  $P_d=1$  (dyne/cm<sup>2</sup>).

Settling velocity,  $W_s$ , of cohesive flocs is calculated with the parameterization by Burban *et al.* (1990) in

which flocculation is dependent on the product of local concentration and vertical shear stress in water column.

$$W_s = \alpha(CG)^\beta, \quad (6.1)$$

$$G = \rho_s K_M \left[ \left( \frac{\partial U}{\partial Z} \right)^2 + \left( \frac{\partial V}{\partial Z} \right)^2 \right]^{1/2}, \quad (6.2)$$

in which  $\rho_s$ : dry density of suspended medium,  $K_M$ : vertical eddy viscosity,  $\alpha$ ,  $\beta$ : the empirical non-dimensional constants,  $W_s$ ,  $C$  and  $G$  are expressed in m/day, mg/L, and dyne/cm<sup>2</sup>, respectively. The above equation implicitly incorporates the effect of internal shear stress,  $G$ , on aggregation and settling. For saltwater suspensions, Burban *et al.* (1990) estimated values of  $\alpha$  and  $\beta$  to be 2.42 and 0.22 (HydroQual, Inc., 2002).

### 3.3 Bed Shear Stress and Vertical Mixing Parameterization

Bed shear stress for sediments is formulated with slightly being modified based on the extended logarithmic law to be:

$$\tau_b = \rho_s C_d |\bar{u}_b| \bar{u}_b, \quad (7.1)$$

$$C_d = \left[ \frac{1}{\kappa} \ln \left( \frac{z + z_0}{z_b} \right) \right]^{-2}, \quad (7.2)$$

where  $\kappa$ : the von Karman constant,  $C_d$ : bed friction coefficient,  $u_b$ : the bottom-most horizontal velocity vector,  $z + z_0$ : height of  $u_b$  relative to the bed,  $z_0$ : the roughness height, and  $z_b$ : the roughness height for sediments. Together with Eqn. (7), leaving the determination of  $l$  unchanged, where  $l$  is turbulent macroscale,  $K_M$  and the vertical eddy diffusivities  $K_H$  and  $K_q$  must be slightly altered as proposed in Uchiyama (2004) so that:

$$\left. \begin{aligned} K_M &= S_M q(l + \kappa z_0) \\ K_H &= S_H q(l + \kappa z_0) \\ K_q &= S_q q(l + \kappa z_0) \end{aligned} \right\}, \quad (8)$$

where  $S_M$ ,  $S_H$ , and  $S_q$  are the stability functions, and  $q$  is the square root of TKE multiplied by 2, used in the Mellor-Yamada level 2.5 sub-model in POM.

### 3.4 Bed Elevation Modeling

Bathymetry changes can be evaluated from the volume conservation of sediments at the bed varying with erosion and deposition rates computed in the model.

$$\frac{d h_b}{d t} = \frac{1}{\lambda_s \rho_s} (E_r - D_p) \quad (9)$$

where  $h_b$ : bed elevation,  $\lambda_s$ : porosity of the bed sediments. Although the previous studies have often introduced a ‘‘layered’’ bed model (Hayter, 1983; McDonald and Cheng, 1997; HydroQual, Inc., 2002) to incorporate consolidation of deposited sediments and vertical distribution of the dry density of sediments in the bed and the critical shear stress into the numerical models (Tsai and Lick, 1987; MacIntyre *et al.*, 1990), it contains many unknown, tuning parameters. In the present study, the bed elevation model is simplistically formulated to avoid intricate uncertainty.

## 4. RESULTS

### 4.1 Cohesive Sediment Concentrations

The horizontal grid alignment of San Francisco Bay is displayed in **Figure 2**. A total of 45 x 160 horizontal cells and 10 vertical  $\sigma$ -layers are defined in the simulation as used by Uchiyama (2004). Astronomical tidal oscillations are imposed on the open boundary condition off Golden Gate (the bay mouth). Neither fluvial sediments nor surface wind stresses are assumed in the computation for the simplicity. The elevation condition is applied to the open boundary; a spatial gradient (the first order differentiation) of elevation, velocities,  $q^2$ ,  $q^2 l$ , and  $C$  are set to be zero. The hydrodynamic, sedimentological and numerical parameters used in the simulation are listed in **Tables 1** and **2**. The sedimentological parameters employed here are generally standard values, not calibrated with field data since the simulation solely considers tidal currents, so it would have almost no meaning to compare with the observed data quantitatively. Nevertheless, the computed spatial distribution of sediment concentrations and morphological variations indicate a fairly reasonable agreement with the observed results as demonstrated later.

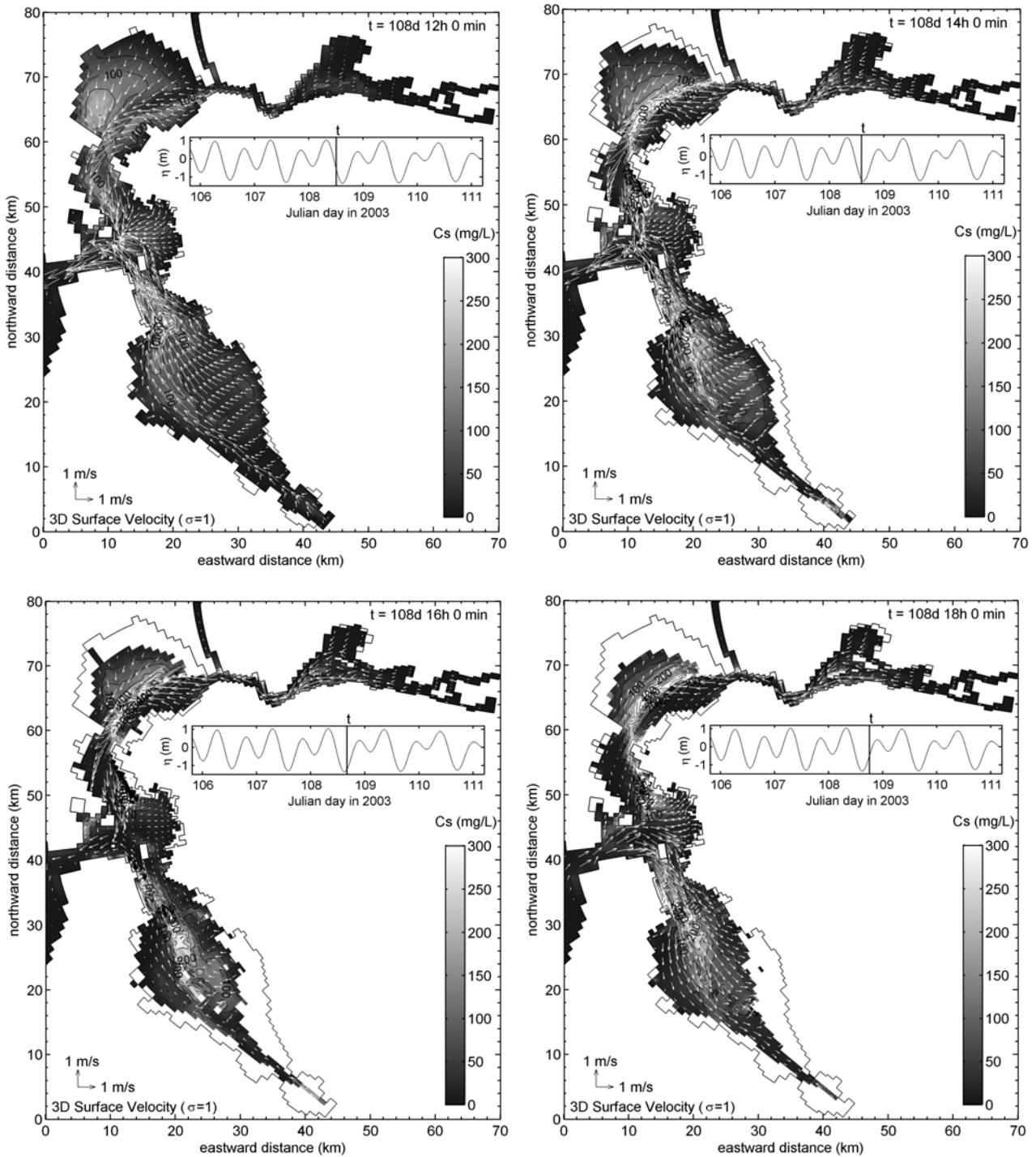


**Figure 3:** Bihourly evolution of the cohesive sediment concentrations (black-white colors) and 3D horizontal velocity vectors (white arrows) at the first  $\sigma$ -layer (surface) during an ebbing phase in a spring tide on the 108<sup>th</sup> and 109<sup>th</sup> Julian day in 2003 (UTC). The contour intervals are set to be 50mg/L.

The starting date of the simulation coincides with March 29, 2003 (the 88th Julian day in 2003) and a simulation *spin-up* (McDonald and Cheng, 1997) is conducted for the first 12 days to attain a dynamically equilibrium distribution of the sediment concentrations since

the simulation starts with zero concentration in the whole domain at  $t=0$ s. The last 28 days (i.e., two spring-neap cycles) are utilized in the following analysis, and thus the total duration of the computation is 40 days. Water surface elevations and 3D tidal current velocities at mul-

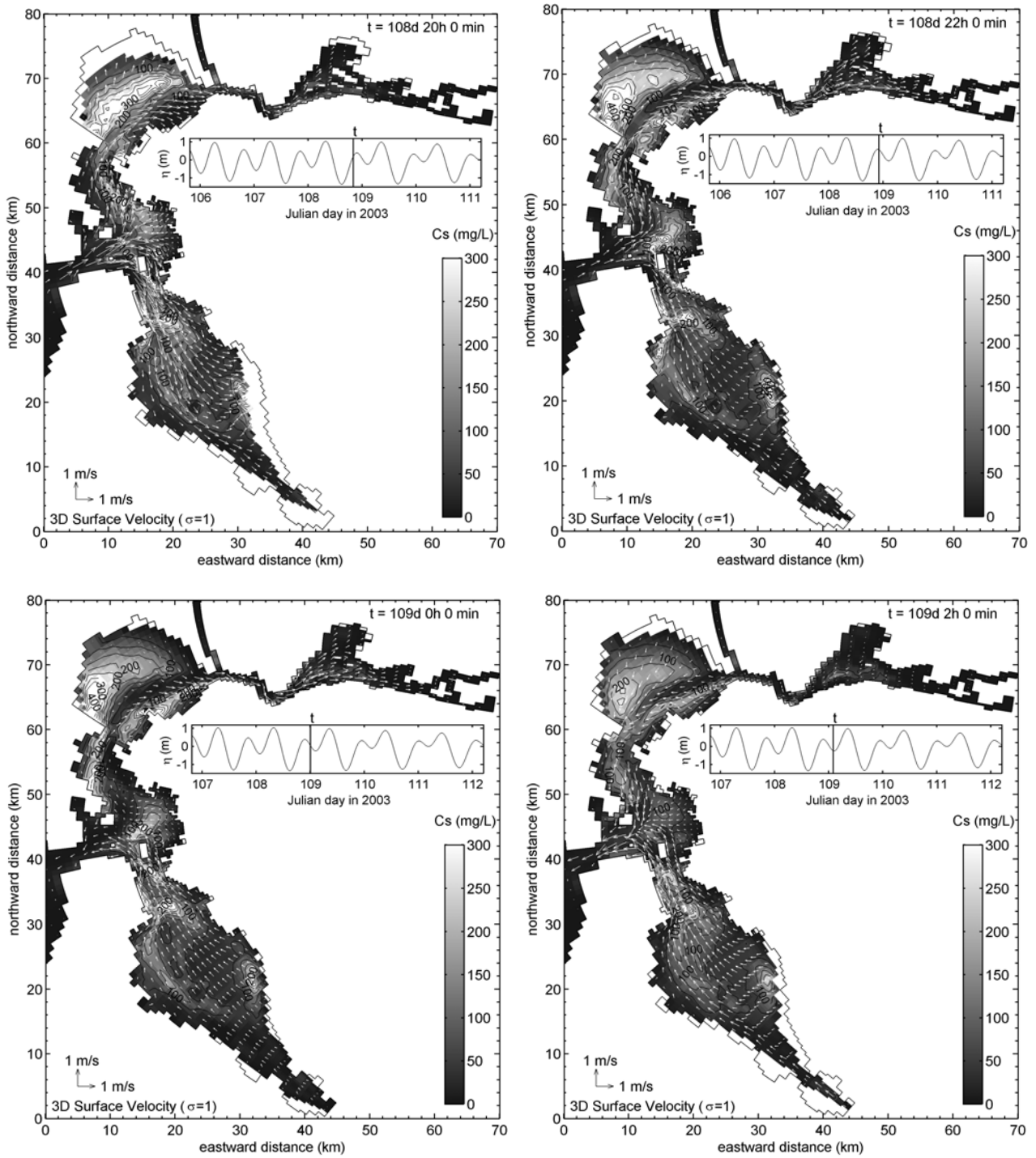


**Figure 4:** Same as **Figure 3**, but during a flooding phase.

multiple locations along the coast line of San Francisco Bay have already validated with the observed data to represent that WD-POM is able to accurately reproduce the hydrodynamics in the whole bay (Uchiyama, 2004).

**Figures 3 and 4** show the bihourly development of the sediment concentrations and the 3D horizontal current velocity vectors at the first  $\sigma$ -layer for 14 hours on the 108th to 109th Julian day in 2003 in UTC. The model outputs exhibit that during a spring tide, cohesive

**Table 3:** Statistical summary of the near-bottom suspended sediment concentrations measured in San Francisco Bay observed by USGS (Buchanan and Ruhl, 2001). The locations of the measurement sites are plotted in **Figure 1**. The concentrations are measured by optical backscatterance sensors (OBSs) calibrated with sampled turbid waters.

Site	mean (mg/l)	median (mg/l)
Mallard Island	46	58
Carquinez Bridge	203	297
Mare Island Causeway	186	235
Channel Marker 9	213	263
Point San Pablo	81	99
Pier 24	33	38
Channel Marker 17	171	215
Dumbarton Bridge	150	190
San Mateo Bridge*	60	73

\* mid-depth concentration

sediments are suspended dominantly in the deeper channels while being transported and deposited on the intertidal areas fringing the bay at flooding phases. This tendency can also be observed during neap tides although magnitude of the variations is much smaller (not shown here) than those for the spring tides. In South San Francisco Bay, the concentrations are not as high as those in San Pablo Bay as weaker tidal currents are generated in South Bay. The sediment concentrations in San Pablo Bay are estimated from the simulation to range from 0 to 300 mg/l while those in South Bay vary about 0-200 mg/l. These ranges of the fluctuations reasonably agree with the observed data as listed in **Table 3** and displayed in **Figure 5**. The measured concentrations range from 0 to 150 mg/l in the whole bay, indicating higher concentrations in San Pablo Bay and Suisun Bay while lower in South Bay. The median concentrations fluctuate from 99 (Point San Pablo) to 297 mg/l (Carquinez Bridge) in San Pablo Bay although in South Bay ranging from 38 (Pier 24, Central Bay) to 215 mg/l (Channel Marker 17, South Bay) as indicated in **Table 3** (after Buchanan and Ruhl, 2001). In addition to the *in situ* measurements, the satellite image analysis gave us the instantaneous surface sediment concentrations as displayed in **Figure 5** (after Ruhl *et al.*, 2001). The image was taken on March 25, 1995, at 13:00, and the concentrations are inferred from the bands-1 and -2 of the NOAA-14 AVHRR, and calibrated with the measured data using optical backscatterance sensors. These observed results clearly support that the

model presented here is capable of realistically reproducing the cohesive sediment concentrations in San Francisco Bay. However, because the concentrations may significantly increase in response to riverine discharges and wind condition, it is necessary to implement these effects into the model in the future.

The incoming tidal waves are propagating as anti-clockwise Kelvin waves but significantly refracted on the intertidal slopes in San Francisco Bay (Uchiyama, 2004) presumably to boost the instantaneous, as well as residual, velocity component normal to the isobaths particularly in the intertidal areas. **Figures 3** and **4** also exhibit that in San Pablo Bay the bed cohesive sediments begin to be resuspended in the channels during an ebbing phase (at 14h), and subsequently being carried in the direction of ebb tidal currents (at 16h through 18h). Next the resuspended sediments appear to be transported onto the intertidal areas in response to the rising tides and to approach the shoreline during floods (at 18h through 22h), and finally the sediments are diluted perhaps by deposition (at 22h though 2h). **Figure 5** shows a similar pattern in which higher concentrations appear to be around the deeper channels although lower on the intertidal shallow areas. This spatial distribution of the sediment concentrations is most likely induced by the tidal current component normal to the isobaths and may provoke specific topography variation in the bay as discussed later.

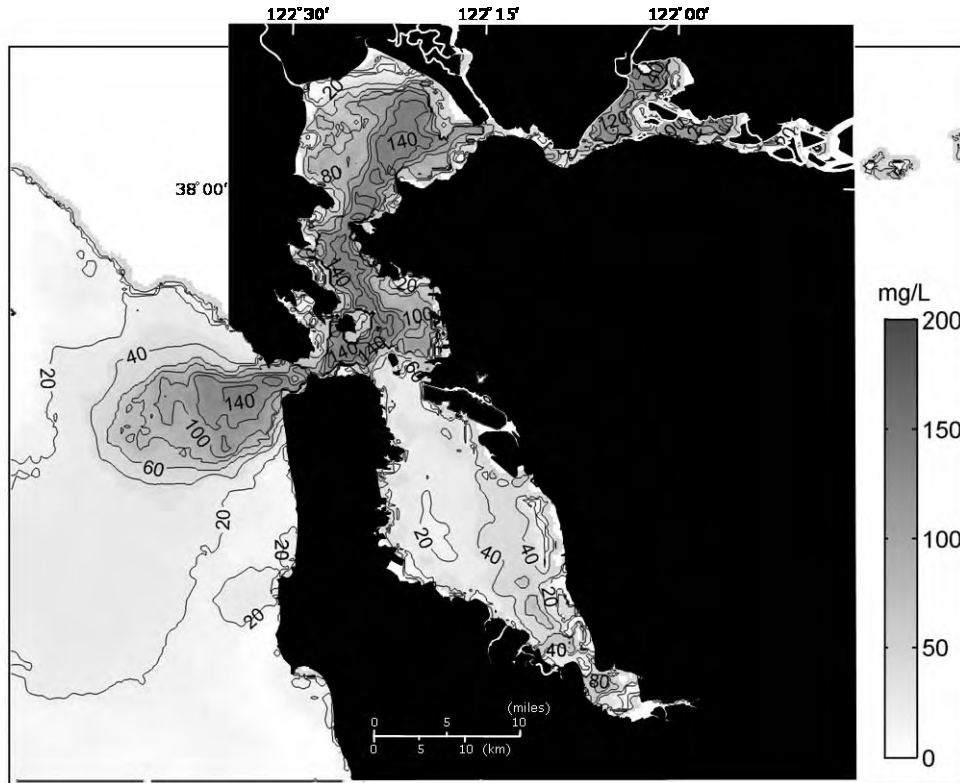


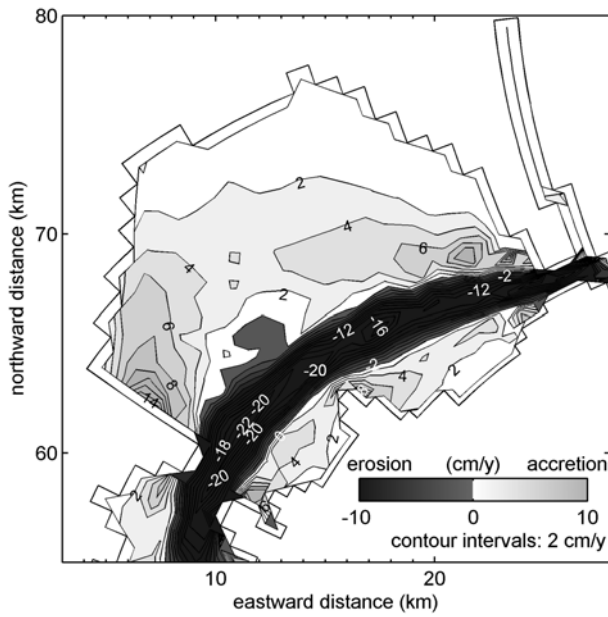
**Figure 5:** A NOAA-AVHRR image corresponding to the instantaneous sediment concentrations in San Francisco Bay on March 25, 1995, at 1300h (after Ruhl *et al.*, 2001).

#### 4.2 Geomorphological Variations

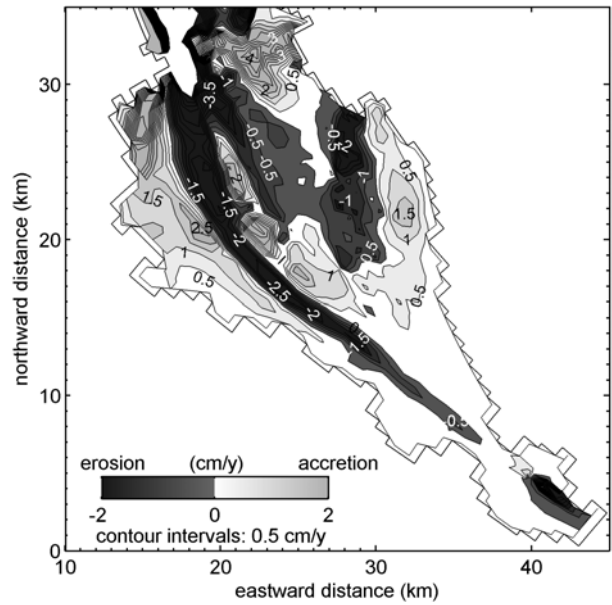
The morphological changes due to the tidal currents during two spring-neap cycles (28 days) in San Pablo Bay and South Bay are estimated as shown in **Figure 6**. Intertidal mudflats tend to slightly be accreted whereas deeper channels seem rather eroded in the both subembayments. This result is obviously consistent with the temporal development of the cohesive sediment concentrations as sequentially indicated in **Figures 3** and **4**. Sediment resuspension is predominant in the deeper channels to generate suspended cohesive sediments, resulting in significant erosion. The sediments are then transported and deposited onto the intertidal areas to enhance accretion.

This computed geomorphological pattern is next compared with surveyed topography variations. **Figure 7 (a)** shows the bathymetry-change rate in San Pablo Bay calculated with the historical bathymetry surveys conducted by COOPS-NOS-NOAA in 1922 and 1951 and summarized by USGS (after Jaffe *et al.*, 1998).

The channel is eroded by about 2.4m for 29 years between two surveys to yield  $\sim 10\text{cm/y}$  as shown in **Figure 7 (a)**. The simulated maximum erosion rate is about 10-20 cm/y, demonstrating the model can qualitatively replicate the geomorphological behavior in San Pablo Bay realistically. This consistency also suggests that the sediment transport and associated bathymetry variations are largely controlled by tidal currents. However, the locations of the most accretive regions inferred by the model outputs are slightly different from those by the surveys, probably because the model neglects the surface wind stress, waves and fluvial discharges, and employs the simplified sediment submodels. Similar comparison can be done by examining **Figures 6 (b)** and **7 (b)** which exhibits bathymetry changes between 1931 and 1956 in South Bay on the basis of the surveys (after Foxgrover *et al.*, 2004). The bathymetry tends to vary at around  $\pm 2\text{-}3\text{cm/y}$  in the simulated results although about  $\pm 1\text{-}2\text{cm/y}$  calculated from the surveys. The model-generated morphological pattern is much different from that evaluated by the surveys. Accretion pre-

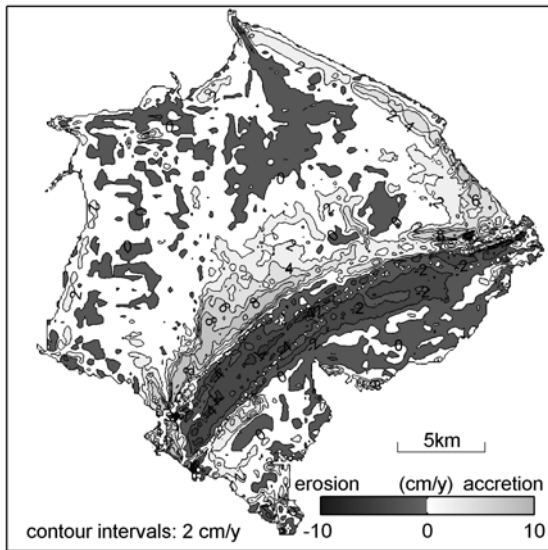


(a) San Pablo Bay – Central San Francisco Bay

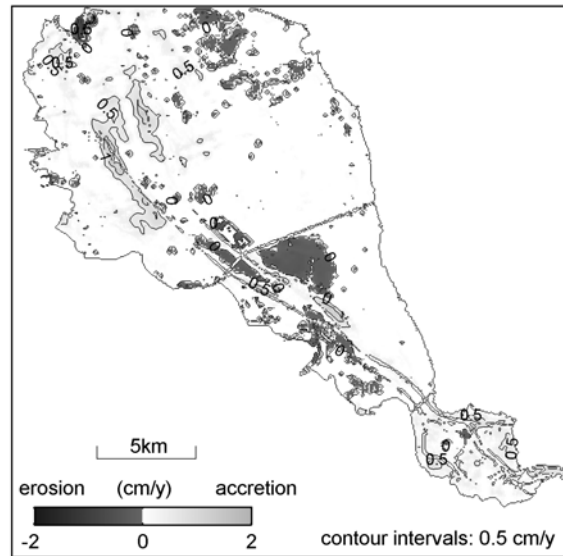


(b) South San Francisco Bay

**Figure 6:** Model-estimated bathymetry changes in (a) San Pablo Bay and (b) South San Francisco Bay.



(a) San Pablo Bay – Central San Francisco Bay



(b) South San Francisco Bay

**Figure 7:** The erosion and accretion rate estimated for the historical bathymetric surveys conducted by CO-OPS, NOS-NOAA in (a) San Pablo Bay (after Jaffe *et al.*, 1998) and (b) South San Francisco Bay (after Foxgrover *et al.*, 2004).

dominantly occurs in the whole South Bay according to the surveyed results, while the model output shows that the intertidal areas are largely eroded. This inconsistency may also be caused by the neglecting hydrodynamic components such as wind and waves which generally enhance erosion.

## 5. DISCUSSION

The model is qualitatively able to estimate the cohesive sediment transport and resultant bathymetry variations with having a realistic agreement with the observed

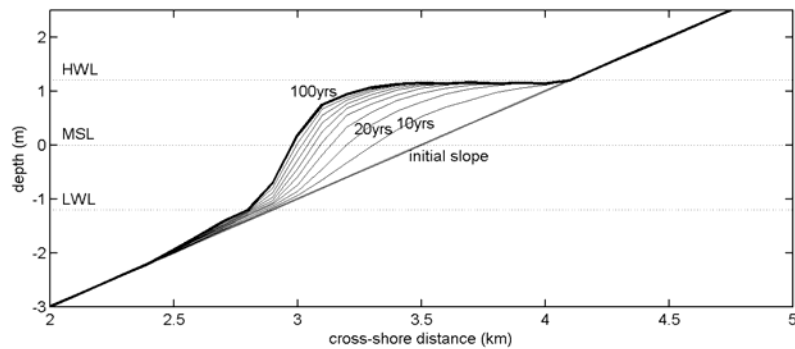


**Figure 8:** Long-term accretion on an intertidal sloping topography. Only a sinusoidal tidal oscillation is considered at the open boundary (the left side).

results. An important finding here is that the tidal currents have a key role in the sediment resuspension, and the subembayment or inter-embayment scale dispersion of the resuspended sediments to induce erosion in the deeper channels and accretion in the intertidal areas. In order to verify this accretive effect of tidal currents on intertidal topography, a 2D-vertical long-term simulation of sediment transport and morphological response on a uniform intertidal slope is performed. The initial beach slope is set at 1:500, and monochromatic sinusoidal tidal oscillations with amplitude of 1.2m and at a period of 12h are imposed on the open boundary condition located at the cross-shore distance of 0km in **Figure 8**. The sedimentological parameters and the other boundary conditions are same as those used in the 3D simulation for San Francisco Bay except the open boundary condition for the sediment concentration. In the 2D simulation, a constant value of  $C_0$  ( $C_0$  is set 100 mg/l here) is used for the sediment concentrations when the direction of currents at the open boundary is landward. The numerical parameters are set here as  $\Delta t_e = 2s$ ,  $\Delta t_i = 60s$ ,  $\Delta x = 100m$ , 5 vertical  $\sigma$ -layers are used, and the Coriolis terms are eliminated.

The computed long-term morphological evolution is found to be similar to the results of the 3D simulation. The flooding tides evidently amplify the shoreward sediment transport to be deposited near the shoreline, and accordingly enhance the accretion in the intertidal areas. As a consequent, the intertidal topography is developed gradually near the high water mark. The cross-shore topography after 100 years is resemble the results

with more simplified 1D models proposed by Roberts *et al.* (2000) and Pritchard *et al.* (2002). This result also suggests that tidal currents evidently influence to raise the sediment deposition on the intertidal areas and to create the flat topography near the shoreline.

## 6. CONCLUSIONS

Cohesive sediment transport and resultant bathymetry response in estuaries encompassed by intertidal area are developed on the basis of WD-POM. The primary advantage of the model is its ability to simulate the vertical hydrodynamics (vertical profiles of 3D velocities, turbulence, sediments, and other passive scalars) even though the water surface descends to become extremely shallow. The model employs the widely-used parameterizations involving the erosion rate submodel by Krone (1962), the deposition rate submodel by Partheniades (1992), and the settling speed submodel by Burban *et al.* (1990).

The model is applied to San Francisco Bay, CA, USA, which is fringed by extensive intertidal mudflats. The model outputs are compared to the observed results by Buchanan and Ruhl (2001), Ruhl *et al.* (2001), Jaffe *et al.* (1998), and Foxgrover *et al.*, (2004) to exhibit a reasonable agreement. The simulated results indicate that the sediments are remarkably suspended in the deeper channels while deposited on the intertidal fringes. This sediment transport induces significant erosion in the channel and visible accretion in the intertidal mudflats. The intertidal areas play an important role in the sediment budgets in the estuary, acting as ‘sink’ of the sus-

pended cohesive sediments under action of the tidal currents. A supplemental 2D vertical simulation with a simplified numerical setting also supports the results deduced from the 3D simulation to demonstrate that tidal currents have evident influence on transporting the re-suspended sediment shoreward and enhancing accumulation to create mudflat topographies.

## ACKNOWLEDGEMENTS

This research project was partially supported by Japan Society for Promotion of Science and is a part of the author's work during his stay at University of California, Berkeley, USA, since March 2002 till March 2004. The author would like to express sincere appreciation to Professor Mark T. Stacey of UC Berkeley, Professor Rodney J. Sobey of Imperial College of London, UK, and Mr. Yasuyuki Nakagawa of Port and Airport Research Institute, Japan, for their helpful comments on the manuscript. Thanks are also due to Mr. Satoshi Inagaki of Kajima Corporation, Dr. Jeremy D. Bricker of Kobe University, Dr. Stefan A. Talke and Dr. David K. Ralston of UC Berkeley for their discussion on the numerical modeling and help with searching for the literatures.

(Accepted on November 10, 2004)

## REFERENCES

- Ariathurai R. and Krone, R.B., 1976. Mathematical modeling of sediment transport in estuaries, *Circulation, Sediments and Transfer of Material in the Estuary*, Wiley, M.L. (ed), *Estuarine Processes*, 11, Academic Press, New York, USA, 98-106.
- Asmus, R.M., Jensen, M.H. Jensen, K.M., Kristensen, E., Asmus, H. and Wille, A., 1998. The role of water movement and spatial scaling for measurement of dissolved inorganic nitrogen fluxes in intertidal sediments, *Estuar. Coast. Shelf Sci.*, 46: 221-232.
- Barros, A.P. and Baptista, A.M., 1989. An Eulerian-Lagrangian model for sediment transport in estuaries, In: *Estuarine and Coastal Modeling*, M. Spaulding (ed.), ASCE, 1: 102-112.
- Black, K.S., Tolhurst, T.J. Paterson, D.M., and Hagerthey, S.E., 2002. Working with natural cohesive sediments, *J. Hydr. Eng.*, 128: 2-8.
- Blumberg, A.F. and Mellor, G.L., 1983: Diagnostic and prognostic numerical circulation studies of the South Atlantic Bight, *J. Geophys. Res.*, 88: 4579-4593.
- Blumberg, A.F. and Mellor, G.L., 1987. A description of a three-dimensional coastal ocean circulation model, In: *Three-dimensional Coastal Ocean Models*, Vol.4, Heaps, N. (ed.), Ameri. Geophys. Union, Washington D.C., pp.208.
- Bricker, J.D., Inagaki, S. and Monismith, S.G., 2004. Modeling the effects of bed drag coefficient variability under wind waves in South San Francisco Bay, *Proc. 8th Int'l Conf. Coastal and Estuarine Modeling*, ASCE, Monterey, CA, USA. (in print, Pers. Comm..)
- Buchanan, P.A. and Ruhl, C.A., 2001. Summary of suspended-sediment concentration data, San Francisco Bay, California, Water Year 1999, *Open-File Report 01-100*, U.S. Geological Survey, Sacramento, CA, USA, 40pp.
- Burban, P.Y., Xu, Y., McNeil, J. and Lick, W., 1990: Settling speeds of flocs in fresh and sea waters, *J. Geophys. Res.*, 95, 18213-18220.
- Cabrera, M.T. and Brotas, V., 2000. Seasonal variation in denitrification and dissolved nitrogen fluxes in intertidal sediments of Tagus estuary, Portugal, *Mar. Ecol. Progress Ser.*, 202: 51-65.
- Casulli, V. and Cattani, E., 1994. Stability, accuracy and efficiency of a semi-implicit method for three-dimensional shallow water flow, *Computers and Mathematics with Application*, 27: 99-112.
- Cheng, R.T., Casulli, V. and Gartner, J.W., 1993. Tidal, residual, intertidal mudflat (TRIM) model and its application to San Francisco Bay, California, *Estuar. Coastal Shelf Sci.*, 36: 235-280.
- Christensen, B., Vedel, A. and Kristensen, E., 2000. Carbon and nitrogen fluxes in sediment inhabited by suspension-feeding (*Nereis diversicolor*) and non-suspension feeding (*N. Virens*) polychaetes, *Mar. Ecol. Progress Ser.*, 192: 203-217.
- Christie, M.C. and Dyer, K.R., 1998. Measurements of the turbid tidal edge over Skeffling mudflats, In: Black, K.S., Patterson, D.M. and Cramp, A. (eds.), *Sedimentary processes in the intertidal zone*, Geological Society, London, UK, 139: 45-55.

- Conomos, T.J., Smith, R.E. and Gartner, J.W., 1985. Environmental setting of San Francisco Bay, *Hydrobiologia*, 129: 1-12.
- De Jonge, V.N. and van Beusekom, J.E.E., 1995. Wind- and tide-induced resuspension of sediment and microphytobenthos from tidal flats in the Ems estuary, *Limnol. Oceanogr.*, 40: 766-778.
- Dyer, K.R., 1986: Intertidal areas, In: *Coastal and Estuarine Sediment Dynamics*, John Wiley & Sons Ltd., Chichester, UK, 260-264.
- Dyer, K.R., 1998. The typology of intertidal mudflats, In: Black, K.S., Patterson, D.M. and Cramp, A. (eds.), *Sedimentary processes in the intertidal zone*, Geological Society, London, UK, 139: 11-24.
- Foxgrover, A.C., Higgins, S.A., Ingraca, M.K., Jaffe, B.E. and Smith, R.E., 2004. Deposition, Erosion, and Bathymetric Change in South San Francisco Bay: 1858 – 1983, *Open-File Report 2004-1192*, U.S. Geological Survey, Santa Cruz, CA, USA, 23pp.
- Galperin, B., Kantha, L.H., Hassid, S. and Rosati, A., 1988. A quasi-equilibrium turbulent energy model for geophysical flows, *J. Atmos. Sci.*, 45: 55-62.
- Gross, E.S., Koseff, J.R. and Monismith, S.G., 1999. Three-dimensional salinity simulations of South San Francisco Bay, *J. Hydraulic Eng.*, 125: 1199-1209.
- Hayter, E.J., 1983. *Prediction of cohesive sediment movement in estuarial waters*, Ph.D. thesis, University of Florida, Gainesville, FL, USA, 363pp.
- Hayter, E.J. and Pakala, C.V., 1989. Transport of inorganic contaminants in estuarial waters, *J. Coastal Res.*, 5: 217-230.
- HydroQual, Inc., 2002. *A primer for ECOMSED, Users Manual*, Ver. 1.3, HydroQual, Inc., Mahwah, NJ, USA, 188pp.
- Inagaki, S., 2000. *Effects of a proposed San Francisco airport runway extension on hydrodynamics and sediment transport in South San Francisco Bay*, Engineer's Degree Thesis, Stanford University, Stanford, CA, USA.
- Jaffe, B.E., Smith, R.E. and Torresan, L.Z., 1998. Sedimentation and Bathymetric Change in San Pablo Bay: 1856–1983, *Open-File Report 98-759*, U.S. Geological Survey, Menlo Park, CA, USA.
- Kerner, M., 1993. Coupling of microbial fermentation and respiration processes in an intertidal mudflat of the Elbe estuary, *Limnol. Oceanogr.*, 38: 314-330.
- Krone, R.B., 1962 : Flume study of the transport of sediment in estuarial processes, *Final Report, Hydraulic Eng. Lab. and Sanitary Eng. Res. Lab., Univ. Calif., Berkeley, CA, USA*.
- Kuwae, T., Hosokawa, Y., and Eguchi, N., 1998. Dissolved inorganic nitrogen cycling in Banzu intertidal sand-flat, Japan, *Mangroves and Salt Marshes*, 2: 167-175.
- Kuwae, T., Kibe, E. and Nakamura, Y., 2003: Effect of emersion and immersion on the porewater nutrient dynamics of an intertidal sandflat in Tokyo Bay, *Estu. Coastal Shelf Sci.*, 57: 929-940.
- Lee, D.H., Bedford, K.W. and Yen, C.J., 1994. Storm and entrainment effects on tributary sediment loads, *J. Hydr. Eng.*, 120: 81-103.
- Li, Y. and Parchure, T.M., 1998. Mudbanks of the southwest coast of India. VI: Suspended sediment profiles, *J. Coastal Res.*, 14 (4): 1363-1372.
- MacIntyre, S., Lick, W. and Tsai, C.H., 1990. Variability of entrainment of cohesive sediments in freshwater, *Biogeochemistry*, 9: 187-209.
- McDonald, E.T. and Cheng, R.T., 1997. A numerical model of sediment transport applied to San Francisco Bay, California, *J. Marine Env. Eng.*, 4: 1-41.
- Mellor, G.L. and Yamada, T., 1982. Development of a turbulence closure model for geophysical fluid problems, *Rev. Geophys. Space Phys.*, 20: 851-875.
- Nakagawa, Y., 2003. Numerical modeling of fine sediment transport processes in the Ariake Bay, Rep. Port and Airport Res. Inst., Port and Airport Res. Inst., Yokosuka, Japan, Vol.42 (4): 25-42. (in Japanese with an English abstract)
- Nakagawa, Y., 2005. Fine sediment transport in Ariake Bay, Japan, *Proc. INTERCOH 2003*. (in print, Pers. Comm.)
- Oey, L-Y., 2005. A wetting and drying scheme for POM, *Ocean Modeling*, 8. (in press, Pers. Comm.)
- Partheniades, E., 1992: Estuarine sediment dynamics and shoaling processes, In Herbick, J. (ed), *Handbook of Coastal and Ocean Engineering*, 3, 985-1071.
- Pritchard, D., Hogg, A.J. and Roberts, W., 2002. Morphological modelling of intertidal mudflats: the role

- of cross-shore tidal currents, *Cont. Shelf Res.*, 22: 1887-1895.
- Ralston, D.K. and Stacey, M.T., 2004. Three-dimensional modeling of intertidal flow and transport: Periodic stratification and its implications for sediment transport, *Suppl. AGU Chapman Conf. Salt-marsh Geomorphology*, Amer. Geophys. Union, Halifax, NS, Canada, 27-28.
- Roberts, W., Le Hir, P. and Whitehouse, R.J.S., 2000. Investigation using simple mathematical models of the effect of tidal currents and waves on the profile shape of intertidal mudflats, *Cont. Shelf Res.*, 20: 1079-1097.
- Ruhl, C.A., Schoelhammer, D.H., Stumpf, R.P. and Lindsay, C.L., 2001. Combined use of remote sensing and continuous monitoring to analyse the variability of suspended sediment concentrations in San Francisco Bay, California, *Estuar. Coastal Shelf Sci.*, 53: 801-812.
- Sheng, Y.P. and Lick, W., 1979. The transport and resuspension of sediments in a shallow lake, *J. Geophys. Res.*, 84 (C4): 1809-1826.
- Shrestha, P.L., Blumberg, A.F. Di Toro, D.M. and Hellweger, F., 2000. A three-dimensional model for cohesive sediment transport in shallow bays, *ASCE Joint Conf. Water Resour. Eng. and Water Resour. Planning and Management*, Minneapolis, MN, USA.
- Siegel, S.W. and Bachand, P.A.M., 2002. Feasibility analysis, South Bay Salt Pond Restoration. *Wetlands and Water Resources*, San Rafael, CA, USA, 228 pp.
- Smolarkiewicz, P.K., 1984. A fully multidimensional positive definite advection transport algorithm with small implicit diffusion, *J. Comp. Phys.*, 54: 325-362.
- Tsai, C.H. and Lick, W., 1987. Resuspension of sediments from Long Island Sound, *Wat. Sci. Tech.*, 21 (6-7): 155-184.
- Talke, S.A. and Stacey, M.T., 2003. The influence of oceanic swell on flows over an estuarine intertidal mudflat in San Francisco Bay, *Estuar. Coastal Shelf Sci.*, 58: 541-554.
- Thomas, W.A. and McAnally, W.H.Jr., 1985. User's manual for the generalized computer program system: open-channel flow and sedimentation, TABS-2, *Instruction Report HL85-1*, US Army Engineer Waterways Experimental Station, Vicksburg, MS, USA.
- Tsuruya, K., Murakami, K. and Irie, K., 1990. Mathematical modeling of mud transport in ports with a multilayer model – Application to Kumamoto Port-, *Rep. Port and Harbour Res. Inst.*, Port and Harbour Res. Inst., Yokosuka, Japan, Vol.29 (1): 3-51.
- Uchiyama, Y., Kuriyama, Y. and Katoh, K., 2001. Suspended sediment and morphological response on Banzu tidal flat, Japan, *Proc.4<sup>th</sup> Int'l Conf. Coastal Dynamics*, Ameri. Soc. Civil Eng., Lund, Sweden: 1038-1047.
- Uchiyama, Y., 2004: Modeling wetting and drying scheme based on an extended logarithmic law for a three-dimensional sigma-coordinate coastal ocean model, *Rep. Port and Airport Res. Inst.*, Port and Airport Res. Inst., Yokosuka, Japan, 43 (4): 3-21.
- Van der Lee, W.T.B., 1998. The impact of fluid shear and the suspended sediment concentration on the mud floc size variation in the Dollard estuary, The Netherlands, In: Black, K.S., Patterson, D.M. and Cramp, A. (eds.), *Sedimentary processes in the intertidal zone*, Geological Society, London, UK, 139: 187-198.
- Van der Lee, W.T.B., 2000. Temporal variation of floc size and settling velocity in the Dollard estuary, *Continental Shelf Res.*, 20: 1495 – 1511.
- Wang, X.H., 2001. A numerical study of sediment transport in a coastal embayment during winter storms, *J. Coastal Res.*, 34: 414-427.
- Wang, X.H., 2002. Tide-induced sediment resuspension and the bottom boundary layer in an idealized estuary with a muddy bed, *J. Phys. Oceanogr.*, 32: 3113-3131.
- Whitehouse, R.J.S. and Mitchener, H.J., 1998. Observations of the morphodynamic behavior of an intertidal mudflat at different timescales, In: Black, K.S., Patterson, D.M. and Cramp, A. (eds.), *Sedimentary processes in the intertidal zone*, Geological Society, London, UK, 139: 255-271.
- Whitehouse, R.J.S., Soulsby, R.L., Roberts, W. and Mitchener, H.J., 2000. Intertidal Processes, In: *Dynamics of estuarine muds*, Thomas Telford, London, UK, 163-168.
- Widdows, J., Brinsley, M. and Elliott, M., 1998. Use of in-situ flume to quantify particle flux (biodeposition rates and sediment erosion) for an intertidal mudflat in relation to changes in current velocity and benthic

- macrofauna, In: Black, K.S., Patterson, D.M. and Cramp, A. (eds.), *Sedimentary processes in the intertidal zone*, Geological Society, London, UK, 139: 85-97.
- Wood, R.G., Black, K.S. and Jago, C.F., 1998. Measurements of preliminary modeling of current velocity over an intertidal mudflat, In: Black, K.S., Patterson, D.M. and Cramp, A. (eds.), *Sedimentary processes in the intertidal zone*, Geological Society, London, UK, 139: 167-175.
- Xie, L., Pietrafesa, L.J. and Peng, M., 2004. Incorporation of a mass-conserving inundation scheme into a three dimensional storm surge model, *J. Coastal Res.*, 20: 282-296.
- Zheng, L., Chen, C. and Liu, H., 2003. A modeling study of the Satilla River Estuary, Georgia. I: Flooding-drying process and water exchange over the salt marsh-estuary-shelf complex, *Estuaries*, 26 (3): 651-669.
- Ziegler, C.K. and Lick, W., 1988. The transport of fine-grained sediments in shallow waters, *Env. Geol. Water Sci.*, 11 (1): 123-132.
- Ziegler, C.K. and Nisbet, B.S., 1994. Fine-grained sediment transport in Pawtuxet River, Rhode Island, *J. Hydr. Eng.*, 120 (5): 561-576.
- Ziegler, C.K. and Nisbet, B.S., 1995. Long-term simulation of fine-grained sediment transport in large reservoir, *J. Hydr. Eng.*, 121 (11): 773-781.